

Performance Analysis of a Small-Scale Master Airscrew Propeller using Experimental and Analytical Methods

Jijo Unnikrishnan¹, Sanjay Ambadi², Pankaj Ghughyal³

¹Staff Instructor, Naval Institute of Aeronautical Technology, Cochin

²PG Scholar, Naval Institute of Aeronautical Technology, Cochin

³PG Scholar, Naval Institute of Aeronautical Technology, Cochin

Abstract – Profound application of custom-made UAVs and MAVs demand selection of small-scale propeller with suitable performance characteristics to meet the desired mission requirements. Different approaches are used towards assessment of performance characteristics namely experimental, analytical, computational, etc. In the present study, the endeavour has been to devise a method to analyse the performance characteristics of a small-scale propeller using both experimental and analytical methods. A propeller test rig has been custom designed for the experimental analysis in the wind tunnel. A specific propeller is selected (Master Airscrew 11"x10") and the experiments have been conducted at multiple values of constant propeller rpm, varying the advance ratios. The propeller performance characteristic of interest in this study has been the thrust produced and its variation against advance ratio. Analytical assessment has been done using the classical Blade Element-Momentum theory. The obtained experimental and analytical results have also been compared with the characteristic data of the particular propeller obtained from UIUC Propeller Database. Result shows that the characteristics are in consonance with the standard trend with minimal acceptable deviation.

KeyWords: Advance Ratio, anemometer, blade angle, chord, coefficient of thrust, Reynold Number, XFOIL, UIUC, UAV, MAV, Master Airscrew, slip stream, vorticity, blade element, inflow factor

1. INTRODUCTION

Various modelling methods have been devised to predict the performance and flow field of the propeller and to design new ones. Momentum theory developed by Rankine [1] and Blade Element Theory (BET) developed by William Froude [2] were the two classical methods prominent in the 19th and early 20th century which were based on two independent line of thoughts [3]. Rankine momentum theory predicted the thrust of a propeller based on the changes in momentum and kinetic energy of the airstream passing through the propeller disc, wherein the thrust generation was purely by virtue of motion of working fluid across the propeller disc. This theory did not explain the manner in which thrust and

torque was transmitted from propeller blades to the working fluid [4].

BET developed by Froude [2] utilized the aerodynamic characteristics of elemental blade sections of a propeller to obtain the resultant lift and drag forces. Lift and drag forces of every elemental blade sections were obtained and summing up of contributions from all the elemental blade sections obtained the resultant lift and drag forces [4]. BET considered the blade sections as 2-dimensional and aspect ratio effects (3-dimensional) and vorticity effects in the slip stream were neglected [3]. Stefan Drzewiecki [5] modified BET and introduced correction terms by incorporating aspect ratio effects for every blade section, but failed to predict the slip stream effects [4].

Continued pursuance resulted in the formulation of Vortex Theory, a derivative of BET, mitigated the drawbacks of BET ie, modelling of vorticity effects [3]. The challenge of vortex theory was to model the vorticity in the propeller slip stream ie, induced velocity by wake. In the vortex theory formulated by Betz, Prandtl [6] and Glauert [7], vorticity in the slip stream was predicted using a wake model i.e using a rigid cylinder and vorticity was transported downstream without contraction of the slip stream. In these methods, the blade loading was considered to be minimum [3]. Following the Betz theory, Goldstein [8] modelled the periodic nature of slip stream by modelling each blade by a single bound vortex with varying circulation in the radial direction. However, Goldstein with his model, could only predict the solution for light loading blades and was inaccurate for small advance ratio blades [3]. Theodorsen [9] further modified Goldstein's theory and developed model for heavily loaded blades including contraction effect of slip stream.

Theory of Theodorsen is a close approximate of real time flow field of propeller, though no universal theory predicts the actual flow field. Different theories are combined as per the flow dynamics towards propeller flow field analysis. Based on these methods, various experimental and

computational techniques have been developed to analyse the propeller performance characteristics.

Selection of a suitable propulsion system to match the desired aircraft performance in various regimes is a critical step during the design stage. Therefore, for a propeller aircraft, selection of an apt propeller with suitable aerodynamic characteristics is of paramount importance. The propeller performance data of conventional aircraft is well documented [10]. Small scale aircraft viz. Unmanned Aerial Vehicle (UAV), Micro Aerial Vehicles (MAV), Radio Controlled (RC) aircraft etc have profound usage in both military and civil applications. They use small scale propeller with diameter less than 24 inches which operate at low Reynold number, low forward speed and high rotor rpm [11] and their performance data is scarce. A database indicating the performance of such small-scale propellers under varying operating conditions will enable the designer to suitably select the propeller of his requirement. Various efforts to develop such database have been attempted.

Brandt et al. [12] conducted experimental studies on Reynold Number effect on small scale propellers with diameter ranging from 9 to 11 inches and propeller speed varying from 1500 to 7500 rpm at University of Illinois at Urbana Champaign (UIUC). The study was conducted on 79 commercially available small-scale propellers for Reynold Number ranging from 50,000 to 100,000. Merchant [13] at Wichita University, USA studied the low Reynold Number effects on 30 small scale propellers with diameter varying from 6 to 22 inches, and at Reynold Number ranging between 30,000 to 300,000. Deters et al. [14] conducted experimental study on 21 types of MAV propellers of diameter ranging from 2.25 to 5 inches. A propeller data base has been formulated at UIUC, called UIUC propeller data base [15], based on experiments conducted on various commercially off the shelf small scale propellers manufactured by APC, Master Airscrew, Graupner etc. The data base enables a ready reckoner for the designers to choose suitable propeller for their propulsion plant.

The scope of the present research is to assess the performance parameters of a small scale commercially available propeller using experimental testing. A test rig was designed and fabricated to conduct wind tunnel tests at various operating conditions of the propeller. The result thus obtained has been validated analytically using Blade Element Momentum Theory. Both the results thus obtained have been further compared with the UIUC data base to validate the accuracy.

A commercially available small-scale fixed pitch, two bladed propeller manufactured by Master Airscrew, GF series 11" (diameter) x10" (pitch), weighing 28.1 grams was selected for the research. The propeller made of Glass Fibre Reinforced Composite had maximum rpm of 15,000. Direction of rotation was counter clockwise when looking from the front. GF series are especially designed in sport flying and in high performance R/C planes with electric motors or glow engine [16].

2. DESIGN AND FABRICATION OF TEST RIG

The purpose of the test rig was to experimentally measure the propeller parameters such as thrust, rpm, forward velocity and advance ratio whilst mounted inside wind tunnel under varying inlet conditions. The method of calculation is based on Momentum theory [1].

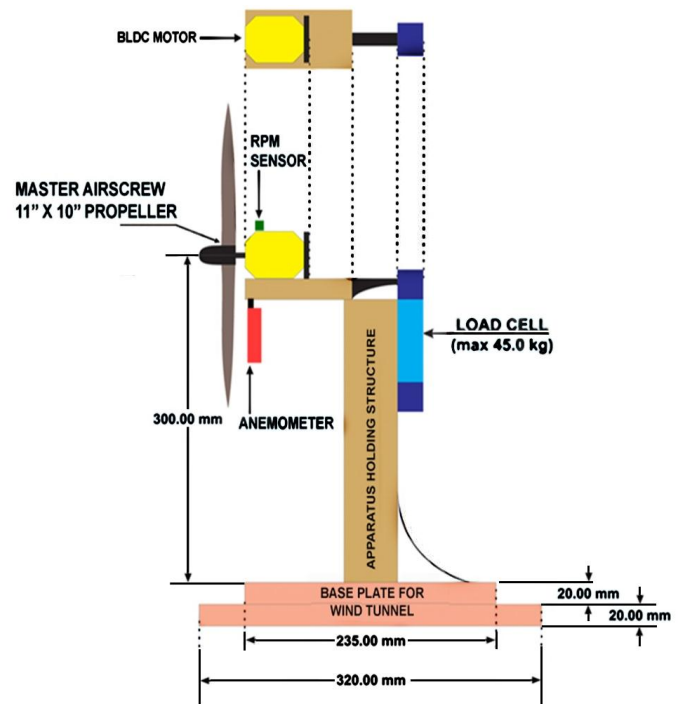


Fig-1: Schematic of Propeller Test Rig

Development of test rig comprised selection of required components, design and fabrication of test stand and integration of components. A schematic diagram of the test rig is shown on figure1. The test rig made of wood consisted of two major parts viz. an instrumented test stand to measure propeller thrust, rpm and forward velocity and a control unit to change propeller rpm and display the readings. While designing the test rig, any rolling/ sliding/ pivot contacts were avoided to reduce measurement error.

2.1 Selection of Components

A brief description of the components selected along with specifications are shown in table 1. Final assembled test rig is shown in figure 2.

1. **Brushless DC Motor (BLDC)** – For the given propeller dimension of 11”x10” with maximum rpm of 15,000, Rimfire 0.46 (42-60-800) GPMG4725 is widely used [17]. The selected BLDC motor had rating of 800rpm/V (kV rating) and high torque/Watt ratio.

2. **Electronic Speed Control (ESC)** – ESC was selected based on the rating of the motor. The max continuous current required and max surge current required for the motor were 60A and 100A respectively. Therefore ESC, Castle Talon 90A rating was selected [18]. The connections and programming of the ESC were undertaken using Talon manual [19].

3. **Battery** –Based on the motor rating of 800 rpm/V and a power factor of 0.8, a battery voltage of 8.6 V (5500/800x0.8) was required. Accordingly, a Li-Po battery (HJ Power) with rating 11.1 V, 2200 AH was selected.

4. **Digital Tachometer** – To measure the propeller rpm, a non-contact type digital photo tachometer (kusam-meco, model-km2234bl) with resolution of 0.1 rpm was used [20]. The sensor was placed on the test stand, behind the propeller.

5. **Anemometer** – Anemometer, model Metrix AVM 01 having a range of measurement varying from 0.3 to 30 m/s was used to measure the forward velocity [21]. The sensor was fitted behind the propeller, above the motor mount as shown in figure (1) and (2).

6. **Load Cell** – Single point off centre load measuring capacity type load cell Rudrra RSL-601 measuring thrust up to 45kgf was used to measure the propeller thrust [22].

	90	90A Max Voltage – 25.2 V Programmable via Castle link USB
Battery	HJ Power	Max Amp – 66 Weight – 184g Capacity – 220 AH Cells – 3
Digital Tachometer	Kusam Meco, KM 2234BL	Sampling time – 1 sec (60 rpm) Resolution – 1 rpm Detecting distance – 50 to 500mm Weight – 235g
Anemometer	Metrix AVM 01	Range – 0.3 to 30m/s Resolution – 0.1 m/s Wind speed accuracy – (+/-0.5) %
Load Cell	Rudrra RSL-601	Composition error – 0.03/0.02 Non-linearity – 0.03/0.017 (%Full Scale (FS)) Repeatability – 0.01 (%FS) Hysteresis – 0.03/0.02 (%FS)

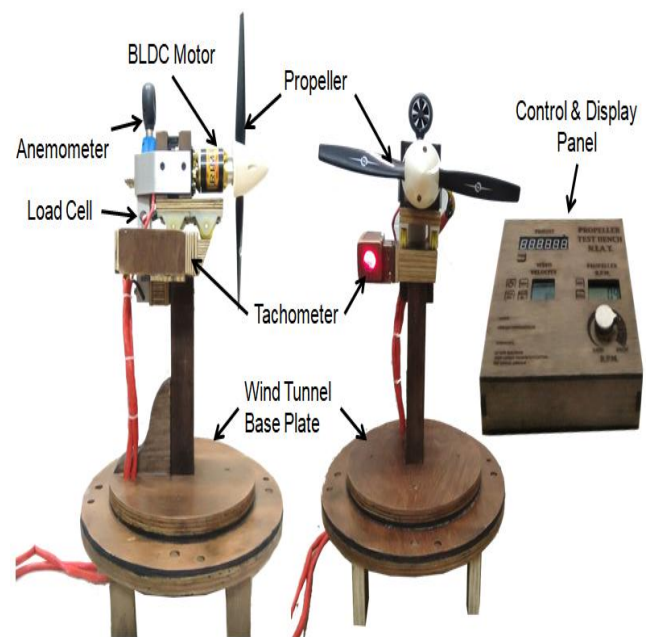


Fig-2: Assembled Test Rig

Table -1: Specifications of Components

Component	Make and Model	Features
BLDC	Rimfire .46 42-69-800 (GPMG4725)	Max Continuous current – 60A Max Surge Current – 100A Rating – 800 rpm/V Weight – 268g
ESC	Castle Talon	Max Continuous Amp –

3. EXPERIMENT AND OBSERVATIONS

3.1 Wind Tunnel

The experiments were conducted at wind tunnel facility of Amrita University, Coimbatore. The wind tunnel was open circuit type with 6:1 contraction ratio, a rectangular test section of 600mmx900mm cross section and length of 2m. The tunnel was run by a 12 bladed axial flow fan of diameter

1.3m. The fan and the tunnel diffuser exit diameters were designed to give maximum wind velocity of 35m/s in the test section. Variable wind speed in the test section was obtained by varying the fan speed. Turbulent intensity was reduced by two anti-turbulent screens of 8 mesh and 16 mesh stainless steel along with the honeycomb of size 50mm x 50mm x 450mm. The turbulent intensity of the tunnel was 15% [23]. Figure 3 shows fitment and mounting of the propeller test rig inside the test section.

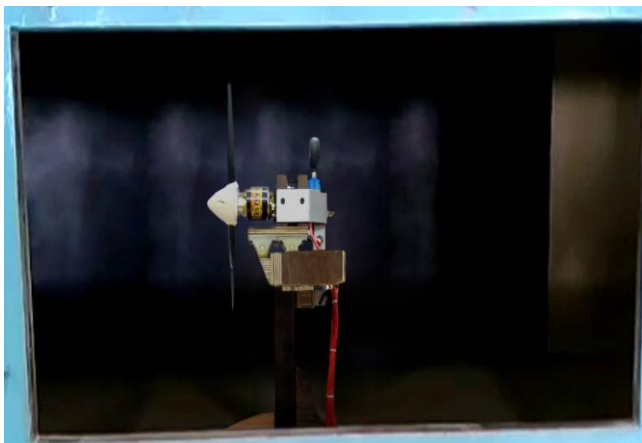


Fig-3: Propeller Test Rig inside wind tunnel

3.2 Experimental Approach - Methodology

Experiment was carried out at different ranges of propeller and wind tunnel RPM combination. The propeller RPM was kept constant and the wind tunnel RPM was varied to get different values of free stream velocity (v_{∞}). v_{∞} was calculated from the Pitot tube fitted in the wind tunnel. The propeller RPM was noted from the digital laser tachometer and was kept constant by adjusting the speed control rheostat. The thrust (T) was noted down from the load cell. The coefficient of thrust (C_T) and advance ratio (J) were calculated using following relations[24]: -

$$v_{\infty} = \sqrt{\frac{2\rho_{ethanol} g\Delta h \sin\theta}{\rho_{air}}} \quad \text{----- (1)}$$

$$C_T = \frac{T}{\rho\Omega^2 D^4} \quad \text{----- (2)}$$

$$J = \frac{v_{\infty}}{\Omega D} \quad \text{----- (3)}$$

Here, g is gravity, Δh is manometric head, θ is inclination, Ω is rotating speed of propeller in radians per second, ρ is density, D is propeller diameter.

The experiment was conducted by keeping propeller at

constant RPM and varying free stream velocity. The readings were taken at 3500rpm, 4000rpm and 4500rpm of the propeller. The observed experimental values are mentioned in table 2.

Table -2: Observations

Ω (rpm)	v_{∞} (m/s)	Re $\times 10^5$	T (N)	J
3500	2.56	1.20	2.62	0.16
	5.12	2.40	2.34	0.31
	7.46	3.50	1.99	0.46
	9.74	4.57	1.47	0.59
	11.99	5.63	1.05	0.74
4000	2.56	1.20	3.73	0.14
	5.12	2.40	3.43	0.27
	7.46	3.50	2.95	0.40
	9.74	4.57	2.42	0.52
	11.99	5.63	1.77	0.65
4500	2.56	1.20	4.44	0.12
	5.12	2.40	4.15	0.24
	7.46	3.50	3.88	0.36
	9.74	4.57	3.49	0.47
	11.99	5.63	2.93	0.57

The wind tunnel walls constrict the flow field thereby increasing the static pressure in the propeller slip stream. Thus, propellers in a wind tunnel produce more thrust than the unrestricted flow. The thrust obtained was equal to the thrust corresponding to a lower free stream velocity in an unrestricted flow. The boundary corrections developed by Glauert [25] was incorporated in equation 4 to get the corrected free stream velocity (v'_{∞}).

$$\frac{v'_{\infty}}{v_{\infty}} = 1 - \frac{\tau\alpha}{2\sqrt{1+2\tau}} \quad \text{----- (4)}$$

$$\text{; where } \alpha = \frac{A}{c} \text{ and } \tau = \frac{T}{\rho A v_{\infty}^2}$$

Here, A is the propeller cross section area, C is the wind tunnel cross section area, ρ is the density of air, T is the thrust measured and v_{∞} is the free stream velocity. Corrected advance ratio (J') is obtained from equation 5.

$$J' = \frac{v'_{\infty}}{\Omega D} \quad \text{----- (5)}$$

3.3 Experimental Results

The corrected values, J' and v'_{∞} are depicted in table 3. Variation of T and C_T vs J' is plotted in chart 1 and chart 2 respectively.

Table -3: Corrected velocity and Advance ratio

Ω (rpm)	τ	v'_∞ (m/s)	J'	C_T
3500	5.61	2.33	0.14	0.11
	1.26	4.92	0.30	0.09
	0.50	7.31	0.45	0.08
	0.20	9.65	0.59	0.06
	0.10	11.94	0.73	0.04
4000	7.34	2.29	0.12	0.11
	1.84	4.87	0.26	0.10
	0.74	7.26	0.39	0.09
	0.32	9.60	0.52	0.07
	0.17	11.89	0.64	0.05
4500	9.52	2.25	0.11	0.12
	2.22	4.84	0.23	0.11
	0.98	7.22	0.35	0.10
	0.52	9.54	0.46	0.09
	0.29	11.84	0.57	0.07

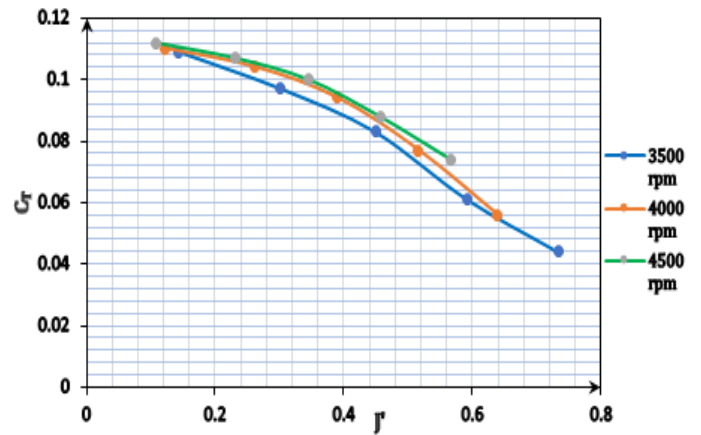


Chart-2: Coefficient of Thrust vs Advance Ratio

4. ANALYTICAL TECHNIQUE

In this part, the thrust estimation of the propeller (Master Aircscrew 11"x10") is undertaken using Blade Element Momentum (BEM) methodology and the result is validated with the experimental values. BEM models have been widely used in design of full-scale wind turbines, helicopter blades and both small and large scale propellers [26].

Here, the propeller blade is divided into elemental sections along the span to determine the aerodynamic loads acting on every section, which is further integrated to obtain the net thrust and torque acting on the blade. A schematic of the propeller stream tube is shown in figure 4. The propeller disk is assumed to be uniformly loaded and therefore the velocity across the propeller disc, $v_\infty + v_1$, is assumed to be constant across the span (v_∞ is the free stream velocity and v_1 is the axial inflow velocity imparted by virtue of propeller rotation). $v_\infty + v_1$ is measured using an anemometer as shown in figure 1. The radial inflow velocity is assumed to be negligible or zero [27].

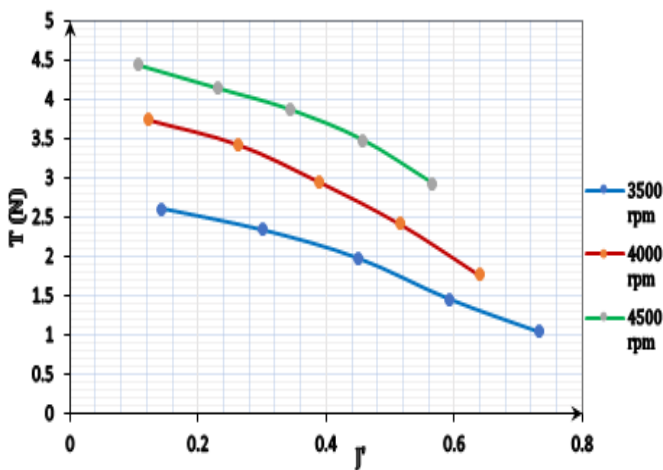


Chart-1: Thrust vs Advance Ratio

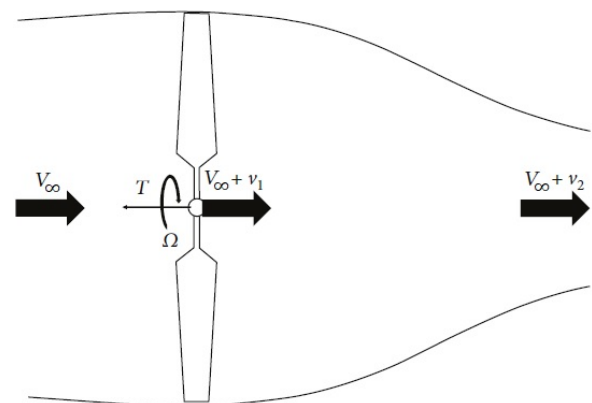


Fig-4: Propeller stream tube [27]

A typical elemental section is a two-dimensional airfoil, and the velocity triangle and aerodynamic forces acting on the blade section is as shown in figure 5.

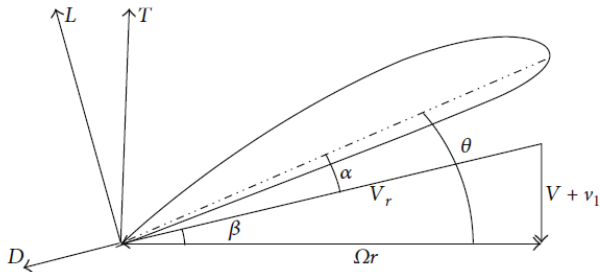


Fig-5: Elemental Blade Velocity triangle [27]

The resultant axial velocity, $V+v_1$ subtends an angle β with the horizontal. The elemental thrust, dT , and total thrust, T , were calculated from the following relations.

$$\beta = \tan^{-1} \frac{(V+v_1)}{\Omega r} \quad \text{----- (6)}$$

$$\alpha = \theta - \beta \quad \text{----- (7)}$$

$$V_r^2 = (V+v_1)^2 + (2\pi r \Omega)^2 \quad \text{----- (8)}$$

$$dT = \frac{1}{2} N \rho C_L (V_r^2 c \cos \beta) dr \quad \text{----- (9)}$$

$$T = \frac{1}{2} N \rho \int_0^R C_L V_r^2 c \cos \beta dr \quad \text{----- (10)}$$

Here, N is the number of blades, V_r is the resultant velocity, c is the elemental chord, r is the elemental location from the hub and C_L is the coefficient of lift of the elemental airfoil.

4.1 Analytical Approach - Methodology

The aerodynamic forces and hence the elemental thrust generated by the propeller blade sections depend on spanwise airfoil geometry. Therefore, understanding the propeller blade profile was prudent to undertake the BEM analysis. Since the profile of the propeller under experiment was unknown, a reverse engineering technique of 3-dimensional scanning was adopted to extract the airfoil sectional geometry [28]. A 3-dimensional model of the propeller was generated using Hexagon Absolute Arm Industrial scanner, model 8320-6 with RS5 laser scanner with minimum and maximum deviation of 20 microns and 40 microns respectively. The Master Airscrew 11" x 10" propeller along with the scanned images is shown in figure 6.



Fig-6: Propeller Scanned views

The scanned model was divided into four sections as shown in figure 7. The cross section of each of these were measured and aerofoil profiles with the geometry closest to these were determined. The identified NACA profiles are shown in figure 8.

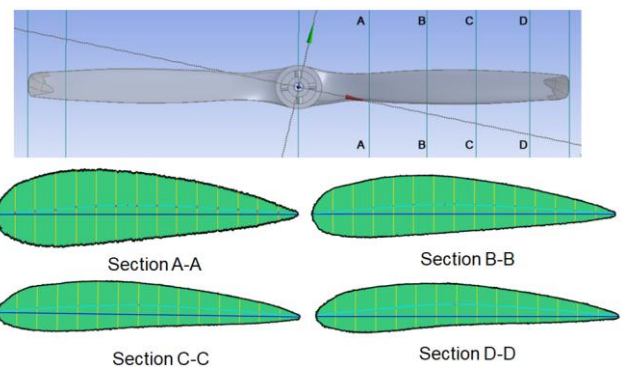


Fig-7: Spanwise propeller cut sections

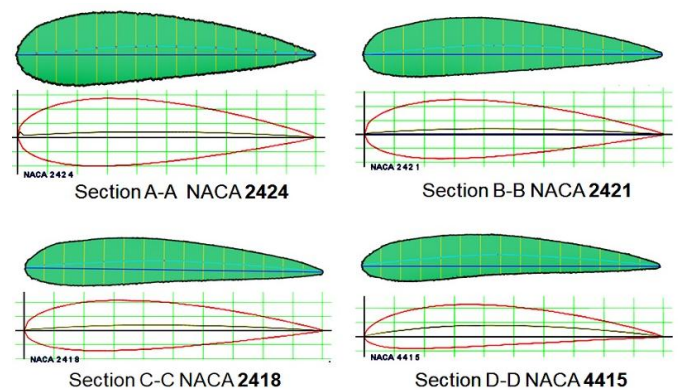


Fig-8: Equivalent NACA profiles

The blade angles (θ) at these sections were obtained from the geometry. The resultant axial velocity, $V+v_1$, was measured using the anemometer. The inflow angle, β , and the angle of attack, α , of every section were calculated using equation 6 and 7 respectively. The coefficient of lift, C_l of the sections were obtained from XFOIL software, version 6.99, which is an interactive program for designing sub sonic airfoil based on panel method to predict the aerodynamic

characteristics. A sample result of one such analysis is shown in figure 9.

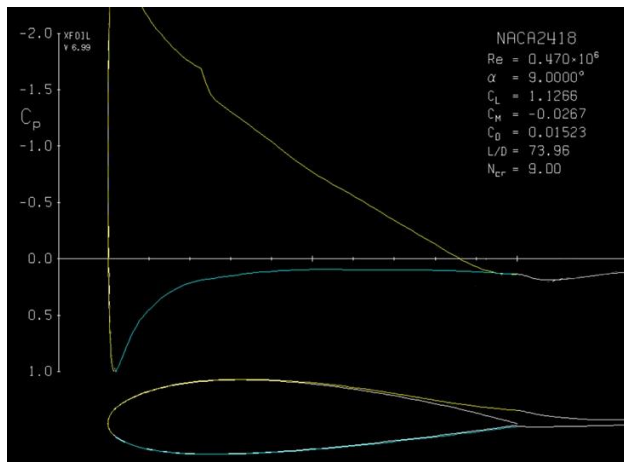


Fig-9: Result of XFOIL Aerofoil analysis

The blade angle (θ) of the sections, its distance from the hub r , and chord c are shown in table 4. The coefficient of lift, C_l for every section for different forward velocities at 4000rpm was obtained from XFOIL software and is shown in table 5. The values of other relevant parameters are shown in Appendix A.

Table -4: Sectional Geometric Parameters

Section	θ (deg)	r (m)	c (m)
A-A	43.7 ⁰	0.0350	0.0215
B-B	31.3 ⁰	0.0660	0.0250
C-C	25.1 ⁰	0.0915	0.0255
D-D	20.1 ⁰	0.1195	0.0220

Table -5: Coefficient of Lift of various sections

v_∞ (m/s)	C_l A-A	C_l B-B	C_l C-C	C_l D-D	Re
2.56	1.2	1.23	1.2	1.37	120149
5.12	0.9	1.11	1.11	1.351	240298
7.46	0.40	1.06	1.03	1.22	350292
9.74	0.11	0.62	0.74	1.08	457514
12	-0.06	0.42	0.54	0.98	563550

4.2 Analytical Results

The resultant velocity, V_r and elemental thrust dT for every section were calculated using equations 8 and 9 respectively and the net thrust, T was obtained by

integrating the elemental thrust along the span of the propeller. Python programming language was used for integration and the code is shown in Appendix B. The net thrust values obtained for different advance ratios for a rotating speed of 4000 rpm is shown in table 6.

Table -6: Analytical Thrust Estimation

v_∞ (m/s)	J	T (N)	C_T
2.56	0.14	3.9	0.13
5.12	0.27	4.14	0.12
7.46	0.40	3.75	0.11
9.74	0.52	2.82	0.09
12	0.65	2.5	0.07

5. RESULT COMPARISON

The thrust estimation of Master Airscrew 11"x10" propeller for various advance ratios at constant operating rpm, obtained using experimental and analytical analyses were compared with UIUC propeller data base of Master Airscrew 11"x10" propeller. The comparative nature of the results is shown in table 7 and chart 3.

Table -7: Comparison of Thrust Estimation

v_∞ (m/s)	J	C_T Exp	C_T Ana	C_T UIUC
2.56	0.14	0.11	0.13	0.12
5.12	0.27	0.10	0.12	0.112
7.46	0.40	0.09	0.11	0.102
9.74	0.52	0.07	0.09	0.088
12	0.65	0.05	0.07	0.068

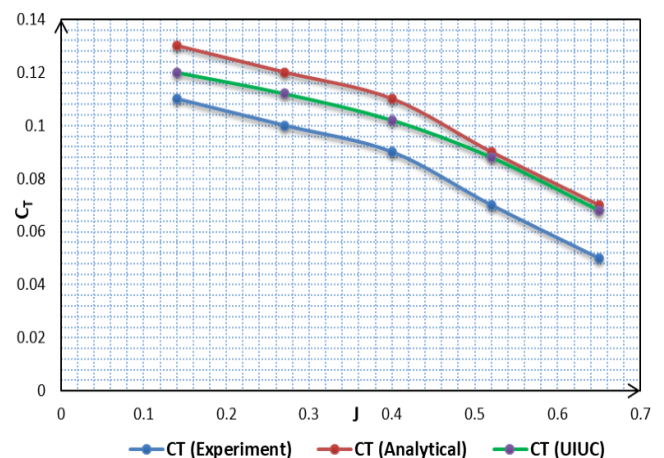


Chart -3: Comparison of Results

6. CONCLUSIONS AND DISCUSSIONS

From the experimental analysis, it is concluded that for a particular propeller rpm, as the forward velocity or advance ratio increases, the thrust coefficient and thrust decreases as indicated in chart 1 and chart 2 and therefore follows the universal trend. Also, for the same forward speed or advance ratio, increase in propeller rpm produces an increased thrust.

As the propeller rpm increases, the thrust produced also increases. This is due to the fact that, with the increase in rpm, the Reynold Number increases which in turn increases the aerodynamic performance. As the Reynolds Number increases, the increase in lift coefficient coupled with reduction in drag coefficient increases the elemental thrust produced by the airfoil, resulting in increase in overall thrust produced by the propeller. Therefore, with the increase in propeller rpm, the thrust increases and the propeller advances more at higher thrust values as indicated in chart 2.

During the experimental testing, the correction applied due to wind tunnel wall effect revealed that the correction factor is prominent at high propeller rpm. With increase in rpm, the propeller slip stream interaction with the tunnel wall increases, resulting in over prediction of the static pressure and thrust as indicated in chart 3.

The analytical technique on the propeller undertaken at 4000 rpm, reveals the same trend of thrust estimation as obtained in experimental analysis for same range of Reynold Number. The over prediction of thrust values at low Reynold Number in analytical method is largely due to the assumptions made, namely, constant axial inflow factor and nil radial inflow factors. The limitation in accuracy of 3-dimensional scanning and prediction of coefficient of lift using XFOIL software may also have contributed to the over prediction.

The calculated values (experimental and analytical) are also found to be comparable with the UIUC propeller data of Master Airscrew 11"x10" propeller as seen in chart 3. The slight under prediction is attributable to the component's efficiency of the propeller test rig, mainly the BLDC motor efficiency.

ACKNOWLEDGEMENT

The authors extend sincere gratitude to Department of Aerospace Engineering, Amrita University, Coimbatore

towards facilitating the wind tunnel facility for experimental testing.

REFERENCES

- [1] W. M. J. Rankine, "On the mechanical principles of the action of the propellers," *Trans. Inst. Naval Arch.*, vol. 6, no. 13, pp. 330–390, 1865.
- [2] W. Froude, "On the elementary relation between pitch, slip, and propulsive efficiency," *Nat. Advisory Committee Aeronautics*, Washington, DC, USA, Tech. Rep. NASA TR-NASA-TM-X-61726, 1920.
- [3] A review of propeller modelling techniques based on Euler methods, GJD Zondervan, published by Delft University Press/1998
- [4] *Aerodynamics Theodore Von Karman First McGraw-Hill paperback Edition*, 1963, ISBN 07-067602-x
- [5] S. Drzewiecki, "Méthode pour la détermination des éléments mécaniques des propulseurs hélicoïdaux," *Bull. L'Assoc. Techn. Maritime*, vol. 3, no. 3, pp. 11–31, 1892.
- [6] A. Betz, "Schraubenpropeller mit geringstem Energieverlust. Miteinem Zusatz von l. Prandtl," *Nachrichten von der Gesellschaft der Wissenschaften zu Göttingen (Mathematisch-Physikalische Klasse)*, vol. 1919. 1919, pp. 193–217.
- [7] H. Glauert, "Airplane propellers," in *Aerodynamic Theory*. New York, NY, USA: Dover, 1963, pp. 251–268.
- [8] S. Goldstein, "On the vortex theory of screw propellers," *Proc. Roy. Soc. London, Ser. A, Math., Phys., Eng. Sci.*, vol. 123, no. 792, pp. 440–465, Apr. 1929, doi: 0.1098/rspa.1929.0078.
- [9] Theodorsen T, "Theory of propellers", McGraw-Hill book company, Inc., 1948
- [10] Kutty, H., and Rajendran, P., "3D CFD Simulation and Experimental Validation of Small APC Slow Flyer Propeller Blade," *Aerospace*, vol. 4, 2017, p. 10
- [11] Venkatesh, B.J. Design and Performance Evaluation of a Propeller; LAP LAMBERT Academic Publishing GmbH & Co. KG: Saarbrücken, Germany, 2012
- [12] Brandt, J.B.; Selig, M.S. Propeller Performance data at low Reynolds numbers. In *Proceedings of the 49th AIAA Aerospace Sciences Meeting*, Grapevine, TX, USA, 7–10 January 2013; pp. 1–18.
- [13] Merchant, M.P. Propeller Performance Measurement for Low Reynolds Number Unmanned Aerial Vehicle

Applications; Wichita State University: Wichita, KS, USA, 2004.

[14] Deters, R.W., Ananda, G.K., and Selig, M.S., "Reynolds Number Effects on the Performance of Small-Scale Propellers," AIAA Aviation and Aeronautics Forum and Exposition (Aviation 2014), AIAA Paper 2014-2151, Atlanta, GA, June 2014.

[15] m-selig.ae.illinois.edu/props/propDB.html.

[16] masterairscrew.com/products/gf-series-11x10propeller

[17] www.hobbyline.com/htm/gpm/gpmgmg4725.htm

[18] www.castlecreations.com/en/talon-90-esc-010-0097-00.

[19] Talon series user guide castle.pdf

[20] www.kusamelectrical.com/df/km-2234bl.pdf

[21] www.metrixinstrument.com/digital-anemometer-avm-01-4173991.html.

[22] www.rudrra.in/pdf/rsl-601.pdf

[23] Wind tunnel operating manual – Amrita University

[24] L J Clancy, "Aerodynamics", Himalayan Books.

[25] Wind tunnel interference on wings, bodies and aircrews by H. Glauert, Aeronautical Research Committee Research and Memoranda No 1566, Sep 1933.

[26] Matthew H Mc Crink and James W Gregory, Blade element momentum modelling of low-Re small UAS electric propulsion system, 33rd AIAA Applied Aerodynamics Conference, AIAA 2015-3296.

[27] Gaurang Gupta and Shaaban Abdullah, Propeller force constant modelling for multi rotor UAVs from experimental estimation of inflow velocity, International Journal of Aerospace Engineering, Vol 2018, article ID 9632942.

[28] R. MacNeill and D. Verstraete, Blade Element Momentum Theory Extended to Model Low Reynolds Number Propeller Performance, 20th Australasian Fluid Mechanics Conference Perth, Australia 5-8 December 2016

APPENDIX A – Analytical Values of different sections

Sec	v_{∞} (m/s)	$V+v_1$ (m/s)	V_r (m/s)	Φ (deg)	α (deg)	C_l
A-A	2.56	10	17.56	34.7	9	1.2
	5.12	11.3	18.77	37	6.69	0.9
	7.46	12.6	19.51	40.21	3.49	0.40

B-B	9.74	14.1	20.15	44.4	-0.69	0.11
	12	15.8	21.65	46.9	-3.15	-0.06
	2.56	10	29	20.16	11.13	1.23
	5.12	11.3	30.44	21.8	9.51	1.11
	7.46	12.6	30.8	24.14	7.15	1.06
	9.74	14.1	30.6	27.43	3.86	0.62
C-C	12	15.8	32.1	29.5	1.79	0.42
	2.56	10	39.05	14.84	10.26	1.2
	5.12	11.3	40.8	16.1	9.01	1.11
	7.46	12.6	41	17.9	7.18	1.03
	9.74	14.1	40.2	20.52	4.57	0.74
	12	15.8	41.8	22.2	2.9	0.54
D-D	2.56	10	50.3	11.47	10.53	1.37
	5.12	11.3	52.4	12.45	9.55	1.351
	7.46	12.6	52.43	13.9	8.1	1.22
	9.74	14.1	51.2	16	6	1.08
	12	15.8	53	17.36	4.64	0.98

APPENDIX B – Python Program for determining thrust by integration

```

from math import cos, pow, sin
import sys
def main():

    b = [43.7, 31.3, 25.1, 20.1]

    c = [0.0215, 0.025, 0.0255, 0.022]

    ra = [0.035, 0.066, 0.0915, 0.1195]

    r = [0.022, 0.0505, 0.0785, 0.107, 0.1405]

    vs = [10, 11.3, 12.6, 14.1, 15.8]
    v1s = [7.45, 6.19, 5.15, 4.36, 3.81]
    cls = ([1.2012, 1.2286, 1.1961, 1.366], [0.9039, 1.1115, 1.111, 1.351], [0.4015, 1.065, 1.027, 1.216], [0.11, 0.6213, 0.7432, 1.0795], [-0.0606, 0.4186, 0.5396, 0.9782])

    ps = ([0.6053, 0.35168, 0.2587, 0.1999], [0.6456, 0.3801, 0.2805, 0.21718], [0.7012, 0.4211, 0.3124, 0.2424],

```

```
[0.7729, 0.4785, 0.3579, 0.2789], [0.8172, 0.5146,
0.3872, 0.3026])
ns = [65.67, 68.16, 67.78, 65.5, 67.33]
eta = [0.25, 0.45, 0.58, 0.68, 0.70]

s = 1
for s in range(1, 6):
    v = vs[s-1]
    v1 = v1s[s-1]
    cl = []
    cl = cls[s-1]
    p = []
    p = ps[s-1]

    n = []
    n = ns[s-1]
    ft = 0.8
    fh = 0.95

    va = v-v1

    def tint(i):

        inti = cl[i] * c[i] * cos(p[i]) * (13.159 * pow(n, 2) *
        ((pow(r[i+1], 3)) - pow(r[i], 3)) - 6.283 * n * v1 *
        cos(p[i]) * sin(p[i]) * (pow(r[i+1], 2) - pow(r[i], 2))
        + (pow(v, 2) + pow(v1, 2) * pow(cos(p[i]), 2) *
        pow(sin(p[i]), 2)) * (r[i+1] - r[i] ))

        return inti

    thrust = ft*fh*1.167 * (tint(0) + tint(1) + tint(2) +
        tint(3))

    print("thrust", s, " is ")
    print(thrust)

    ct = thrust/( 1.167*n*n*0.006059)

    print("CT is ")
    print(ct)

if __name__ == '__main__':
    main()
```